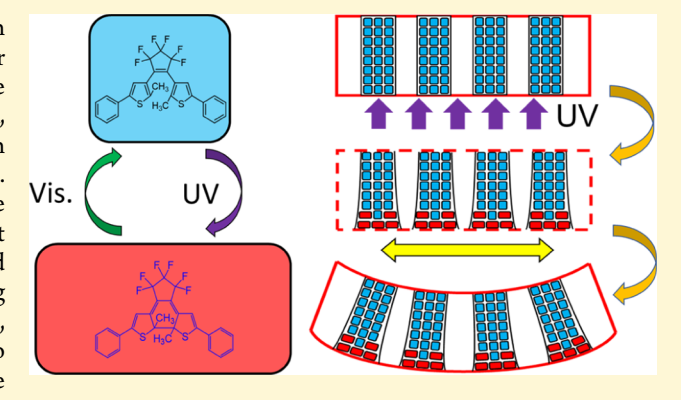


Hybrid Organic-Inorganic Photon-Powered Actuators Based on **Aligned Diarylethene Nanocrystals**

Xinning Dong,[†] Fei Tong,[†] Kerry M. Hanson,[†] Rabih O. Al-Kaysi,[‡] Daichi Kitagawa,*,[†], Seiya Kobatake,*,[§] and Christopher J. Bardeen*,[†]

Supporting Information

ABSTRACT: When photochromic molecules are organized in a crystal, the small-scale forces generated by molecular photoisomerization events can combine together to generate work on micro- or macroscopic length scales. In this work, photomechanical nanocrystals themselves are organized on macroscopic length scales using a porous inorganic template. The organic diarylethene component provides the reversible photoresponse, whereas the porous alumina component provides structural support and directionality. This hybrid organic-inorganic photomechanical material acts as a bending actuator. Using ultraviolet and visible photons as power inputs, as little as 0.1 mg of reacted material generates enough force to tilt a 1.28 g mirror and steer a laser beam. The motion can be cycled multiple times in air and under water. Actuator figures-



of-merit such as energy-to-work conversion efficiency and stiffness are probably limited by the high elastic modulus of the inorganic template, providing an obvious pathway for optimization.

INTRODUCTION

Organic photomechanical materials can transform molecularscale photoisomerization events into a wide variety of mechanical behaviors, including bending, twisting, and coiling. 1-3 Polymer-based materials provide a way to fabricate and pattern photomechanical structures^{4,5} but suffer from low elastic moduli, low-energy density, and slow response times because of the presence of the host polymer. Assembling photochromes into neat molecular crystals avoids the need for a host, and this class of materials can in principle lead to higher energy densities, hardness, and response speed.⁶

When photochromic molecules are assembled into a crystal, their photoisomerization can generate an anisotropic expansion of the crystal lattice (Figure 1a). This lattice expansion, when confined to one side of the crystal, can induce bending as strain builds up between the reactant and product crystal phases (the bimorph or bimetal mechanism).⁷⁻⁹ This mechanism has led to impressive demonstrations of photomechanical molecular crystals that undergo light-induced bending, 8-16 twisting, 17-19 and expansion 20 on microscopic length scales. However, the use of photomechanical molecular crystals in macroscopic actuator structures has been limited for several practical reasons. The

growth of large crystals is difficult and time consuming. Furthermore, large crystals tend to shatter because of internal stress and also suffer from limited light penetration that lowers the total isomerization yield and prevents mechanical motion. 20,21

To make molecular crystals more processable, several groups have explored embedding organic nanocrystals in a polymer matrix to make a composite photomechanical material.²²⁻²⁵ Using several different photochromes, they found that polymer films with embedded photoactive molecular crystals could exhibit bending, but the work generation was not quantified and the mechanical motion was not photoreversible. In these previous attempts, the molecular crystal component typically consisted of random sizes and orientations. Work in the inorganic nanoparticle field has shown that assembly of functional monodisperse nanoparticles into ordered arrays is vital for generating useful collective properties.^{26,27} Thus, a current challenge is to prepare an ordered, monodisperse array

Received: October 30, 2018 Revised: January 8, 2019 Published: January 11, 2019

1016

[†]Department of Chemistry, University of California, Riverside, 501 Big Springs Road, Riverside, California 92521, United States *College of Science and Health Professions-3124, King Saud bin Abdulaziz University for Health Sciences, and King Abdullah International Medical Research Center, Ministry of National Guard Health Affairs, Riyadh 11426, Kingdom of Saudi Arabia §Department of Applied Chemistry, Graduate School of Engineering, Osaka City University, 3-3-138 Sugimoto, Sumiyoshi-ku, Osaka 558-8585, Japan

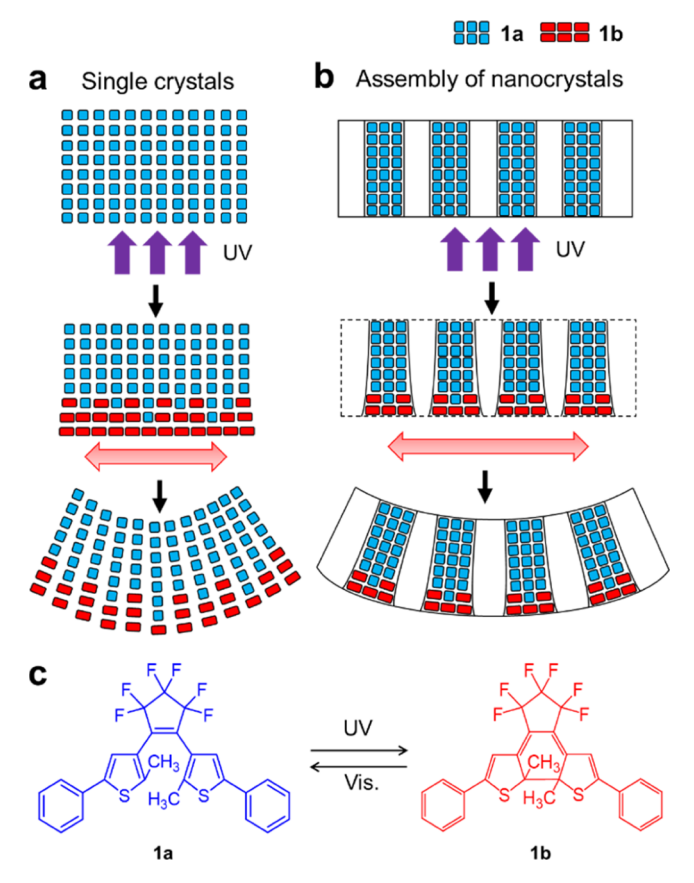


Figure 1. (a) Schematic illustration of how preferential formation of photoproduct on one side of a crystal leads to asymmetric expansion and crystal bending. (b) Porous template allows the creation of an ordered array of crystalline nanowires that can drive bending of the composite structure. (c) Photochemical interconversion between ring-open (1a) and ring-closed (1b) DAE isomers.

of photomechanical organic nanocrystals that can harness the collective motion of the assembly.

The approach taken here is to make a "crystal" of nanocrystals, in which expansion of individual nanocrystals in an ordered array generates internal stress that causes the macroscopic structure to deform. The same bimorph mechanism that leads to mechanical motion in a single crystal (Figure 1a) can be realized on a larger scale through ordered growth of nanocrystals in an inorganic template (Figure 1b), with the template also contributing to the mechanical integrity of the composite. To realize this concept, we chose 1,2-bis(2methyl-5-phenyl-3-thienyl)perfluorocyclopentene (1a), a diarylethene (DAE) derivative that undergoes a unimolecular photoisomerization between its ring-open and ring-closed isomers (Figure 1c) to be the active element. The isomers are thermally stable but can be switched back and forth using UV and visible light for hundreds of cycles. 28-30 The photomechanical behavior of individual DAE microcrystals has been extensively characterized, 18,19,28,29,31-36 and single DAE microneedles are capable of lifting objects 100× more massive than the crystal itself.³² But so far, no one has devised a path that leads from individual microcrystals to macroscopic actuator structures.

■ RESULTS AND DISCUSSION

In this article, we take advantage of the ordering provided by anodic aluminum oxide (AAO) templates, a porous ceramic whose pore diameters and wall thicknesses can be tuned by electrochemical etching conditions.³⁷ To create ordered arrays of 1a nanocrystals, we utilized commercially available Whatman Anodisc templates with a $60 \, \mu \text{m}$ thickness, a nominal pore diameter of 200 nm, and an overall diameter of 12.7 mm that were used as received. A solvent annealing method (Supporting Information Figure S1) was used to facilitate growth of crystalline nanowires of 1a in the AAO channels.³⁸ After crystal growth, the template was mechanically polished to remove excess 1a. When the template was dissolved using concentrated acid, nanowires were obtained (Figure 2a). When

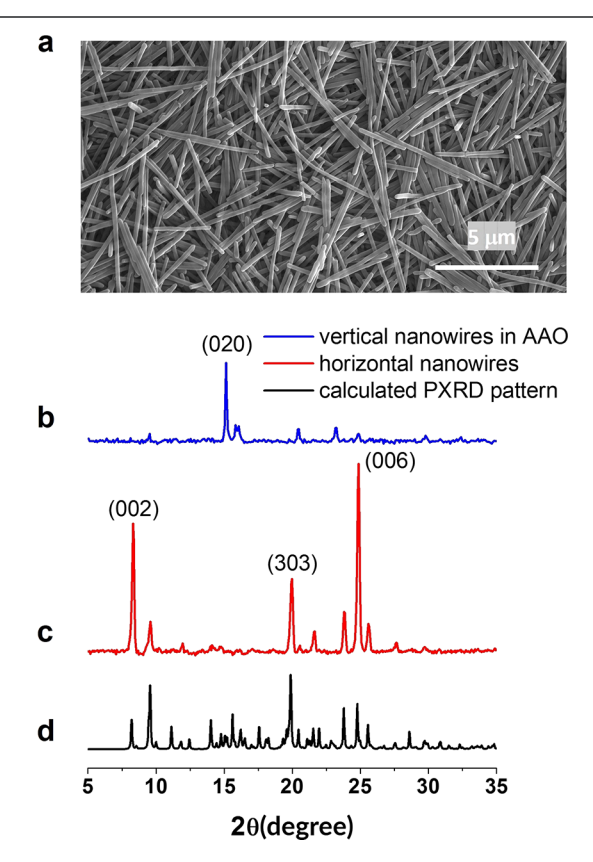


Figure 2. (a) Scanning electron microscopy images of obtained nanowires. (b) PXRD data for vertical DAE nanowires aligned in the AAO template. The dominant (020) peak seen for the vertical nanowires belongs to a Miller plane that is perpendicular to the crystal b-axis, so the b-axis must lie parallel to the nanowire long axis. (c) PXRD data for horizontal nanowires lying on top of an Anodisc filter. The horizontal nanowires exhibit strong (002), (303) and (006) peaks, all corresponding to planes perpendicular to (020) plane. (d) PXRD pattern calculated from the $\bf 1a$ crystal structure.

exposed to 405 nm light, liberated nanowires can reversibly bend and expand, showing that the photomechanical response is preserved in the nanowire form (Supporting Information Figure S2). Polarized light microscopy confirmed that the nanowire bundles consist of oriented crystal domains (Supporting Information Figure S3). Powder X-ray diffraction (PXRD) measurements on intact templates containing vertical nanowires (Figure 2b) show a dominant peak at $2\theta=15^\circ$, corresponding to the (020) Miller plane. This plane runs perpendicular to the crystal *b*-axis shown in Figure 3. Because the PXRD pattern of the intact templates also includes contributions from residual crystallites on the surface, we dissolved the template in $\rm H_3PO_4$ and collected the nanowires

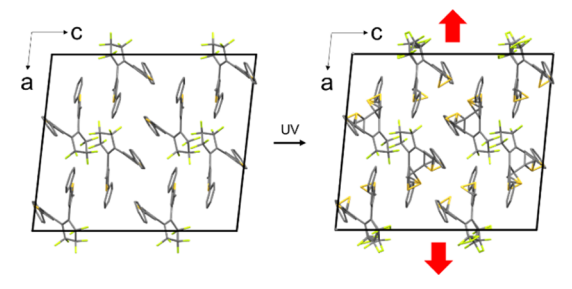


Figure 3. Crystal structure (view along b-axis) of 1a before UV irradiation (left) and crystal structure of a partially converted crystal containing mixture of 1a and 1b after UV irradiation (right). After irradiation, the crystal expands along the a-axis and contracts along the b-axis.

lying flat on an AAO filter surface. The horizontal nanowires showed only peaks corresponding to Miller planes that make right angles to the (020) plane, as expected Figure 2c. Together, these data confirm that 1a preserves its crystal packing and density in the nanowires, which are oriented along the b-axis.

Photoconversion between the two DAE photoisomers can be accomplished using 405 and 532 nm light, wavelengths that correspond to inexpensive, solid-state laser sources. Figure 3 shows that partial conversion of **1a** to **1b** changes the crystal packing and causes a contraction along the *b*-axis and an expansion along the *a*-axis, both on the order of 0.1%.³⁹ There have been no reports of a photomechanical response for macroscopic crystals of **1a**, but we recently found that crystal microribbons composed of **1a** can undergo photoinduced twisting.¹⁹ When one half of a DAE-infuse template was illuminated with 405 nm light, it quickly turned blue (Figure 4a) and diffuse reflectance absorption confirmed creation of

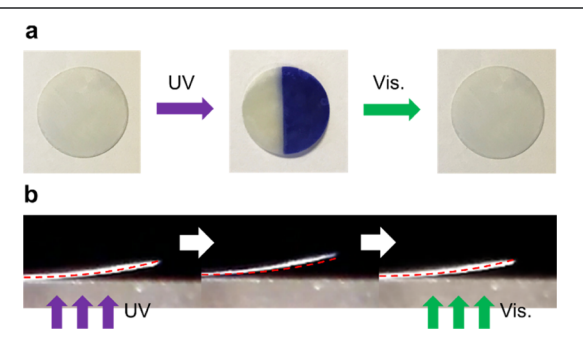


Figure 4. (a) Color change of AAO template after right half is irradiated with UV and then visible light. (b) Reversible template bending after exposure to UV and then visible light. The template is viewed from the side.

the 1b photoisomer (Supporting Information Figure S4). Viewed from the side, the template was also observed to bend, as shown in Figure 4b. Both the color change and bending could be completely reversed after exposure to 532 nm light. The template always bends away from the UV light, and a bend due to bottom irradiation could be canceled out by irradiation of the top to create a balanced bimorph strain (Supporting Information, Figure S5). It is interesting that a macroscopic assembly of nanocrystals exhibits photomechanical bending, whereas macroscopic crystals do not.

Because the photoinduced bending of the template results from the simultaneous deformation of many nanowires, this motion can produce significant amounts of mechanical work. To quantify the work generation as a bending actuator, a two-beam setup (Figure 5a) was used to monitor the ability of the

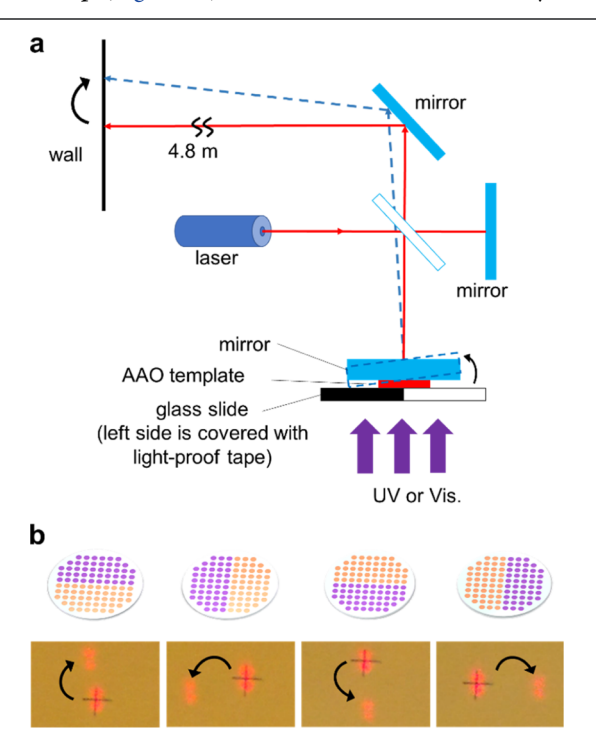


Figure 5. (a) Schematic outline of laser deflection setup. (b) When different regions of the template are irradiated (shown in purple), the mirror tilts in different directions and displaces the beam (dashed blue line) from the reference (red line). The spatial displacement of the spot from the reference spot (marked with a cross) can be used to calculate the vertical displacement of the mirror (Supporting Information).

template to tilt a standard 1 in. diameter mirror and steer a laser beam. Illuminating different quadrants of a single template can tilt a standard 1 in. diameter mirror in any direction and move a laser beam from its reference position (Figure 5b). A laser beam deviation of 0.008 radians allows us to calculate that the mirror edge undergoes a vertical displacement on the order of 100 microns (Supporting Information). Movies of the light-induced mirror motion and laser beam displacement can be viewed as Supporting Information Videos 1 and 2.

The displacement of the beam allows us to calculate an induced template curvature of $2.5 \times 10^{-3}~\rm mm^{-1}$ and an effective expansion of 1.5×10^{-4} for the irradiated side of the template (Supporting Information). This is about $7\times$ less than the molecular expansion along the crystal a-axis as deduced from X-ray crystallographic data on a partially reacted 1a crystal. This small expansion implies less than a $0.1~\rm nm$ change in a $200~\rm nm$ diameter pore and likely results from competition from the expansion/contraction along the a/b-axes, as well as confinement by the AAO template, which will resist the motion of the softer organic component. The molecular interaction with the channel walls is not known, but this will ultimately determine how the organic motion is curtailed by the template.

DAE photochromes are generally resistant to fatigue but can undergo side reactions that generate unreactive byproducts. We found that the DAE-filled templates could undergo

multiple displacement cycles in air, as shown in Figure 6a. The actuation also worked when the template was submerged

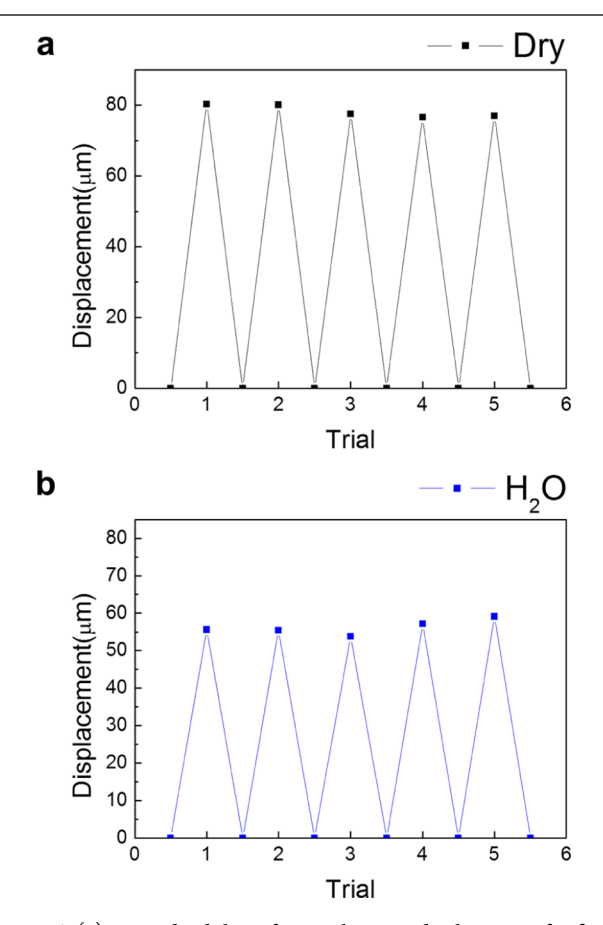


Figure 6. (a) Reproducibility of vertical mirror displacement for five 2 min UV irradiation cycles in air. (b) Reproducibility of vertical mirror displacement for five cycles in water of the same template.

under water, with only a 25% decrease in displacement and no loss of reversibility (Figure 6b). After about 50 cycles in air, a steady decrease in the photoinduced displacement was observed, accompanied by the appearance of a yellow color in the regenerated 1a form. In bulk crystals, 1a can be cycled more than 10⁴ times, ³⁰ so it appears that the hybrid material undergoes accelerated degradation, possibly because of molecular interactions with the AAO walls.

The mechanical displacement closely tracks the photo-isomerization reaction progress (Figure 7a). The linear dependence of the displacement ΔL on the production of 1b allows precise control of the actuator position by controlling the duration of the light exposure. Figure 7b illustrates this control for sequential light exposures. When the light is turned off, the displacement undergoes a slight relaxation by about 5–10% but holds its position afterward. Note that any thermally induced expansion would be expected to completely relax during the off-period, so this observation places an upper limit on the thermal component of the actuation. When the light is turned on again, the displacement starts up where it left off. Under load, the displacement is stable in the absence of light, unlike piezoelectric actuators which require an applied electric field to hold their position.

The photon-to-work conversion efficiency is an important figure-of-merit for photomechanical actuators, but the detailed mechanical analysis of bending actuator structures can be

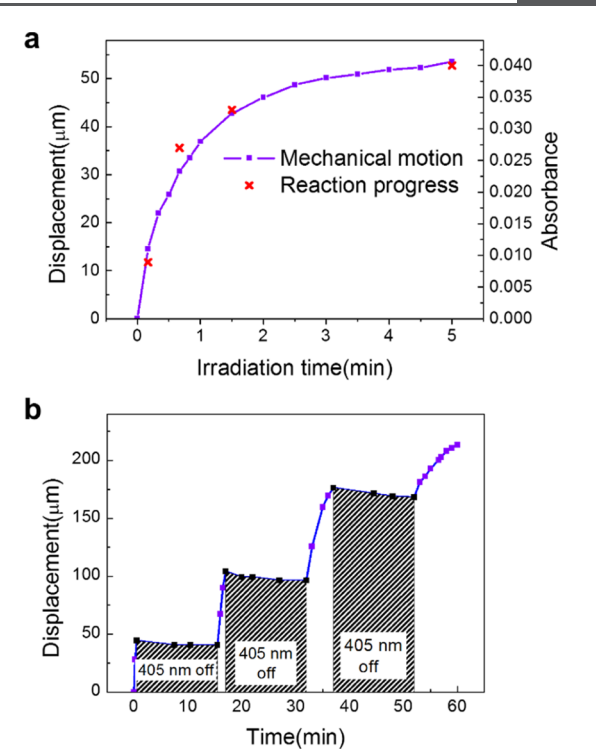


Figure 7. (a) Vertical beam displacement (squares) as a function of 405 nm irradiation time and absorbance of ring-closed isomer 1b (\times). (b) Displacement versus time with 405 nm light turned on and off. The displacement is stable when the illumination is removed.

complicated. 41-43 The macroscopic samples used here allow this conversion efficiency to be measured simply in terms of a mass moved against gravity. Starting with a total mass of 1.6 mg of DAE in the template, a maximum conversion yield of 6.7% was measured by solvent extraction (Experimental Section). This means that 1×10^{-4} g of reacted DAE could generate enough force to lift a 1.28 g mirror, a mass ratio comparable to the best photothermal elastomer system.⁴⁴ From a typical beam displacement, we can calculate that the center of mass of a 1.28 g mirror was lifted by 5.5×10^{-5} m, for a total of 6.9×10^{-7} J of mechanical work. Given that 6.7% of the 1a molecules is converted into 1b, we calculate that $1.22 \times$ 10¹⁷ 405 nm photons were absorbed (assuming an isomerization quantum yield of 1.0^{39}), with a total energy of $5.98 \times$ 10⁻² J. The (absorbed photon)-to-work efficiency is calculated to be 1.15×10^{-5} . This efficiency is comparable to what has been observed for photothermal bending actuators 45,46 but less than that deduced for liquid crystal elastomer bending systems. 41,47 If we consider the input energy to be the total number of incident photons, rather than just the absorbed photons, after 2 min under 7.05 mW/cm², we obtain an (incident photon)-to-work efficiency of 6.15×10^{-7} . These efficiencies represent the first quantitative estimate of the lightto-work conversion efficiency for a molecular crystal photomechanical actuator and provide a well-defined starting point for future optimization.

In most cases, the efficiencies of photomechanical polymer systems have been evaluated in terms of unloaded bending or contraction. Our actuator structure generates an expansion that lifts a load. In this sense, it acts like a bending piezoelectric actuator and it is instructive to evaluate it in terms of parameters commonly used for commercial piezoelectric actuators. This class of actuators is characterized by the

maximum load they can move, known as the blocking force $F_{\rm block}$, and their maximum displacement ΔL_0 in the absence of a load. The ratio of these two parameters gives the actuator stiffness $K_{\rm A}=\frac{F_{\rm block}}{\Delta L_0}$. The stiffness defines the linear relation

between displacement and force generation, $\Delta L = \Delta L_0 - \frac{F}{k_{\rm A}}$. By varying the load on top of the bending AAO template, we can measure the displacement (ΔL) versus force (F) curves shown in Figure 5c. The ΔL versus loading force F curves are fit using an exponential function

$$\Delta L = \Delta L_0 e^{-F/F_{\text{block}}} + y_0 \tag{1}$$

These fits yield R^2 values of 0.96 or greater for all templates measured, which all yielded exponential —force decays (Supporting Information, Figure S6). If we linearize these curves, $\Delta L \cong \Delta L_0 \left(1-\frac{F}{F_{\rm block}}\right)$, we can extract values for $\Delta L_0 = 0.16 \pm 0.08$ mm, $F_{\rm block} = 0.035 \pm 0.006$ N, and $k_{\rm A} = 0.25 \pm 0.10$ N/mm. For comparison, commercially available piezoelectric bending actuators have $\Delta L_0 = 0.1$ –0.5 mm and $F_{\rm block} = 1$ –5 N, $^{48-50}$ leading to $k_{\rm A}$ values ranging from 2 to 100 N/mm. Our photomechanical actuators have comparable ΔL_0 values but $F_{\rm block}$ values that are approximately 100× lower, leading to stiffness values that are also about 100× lower.

Our composite photomechanical actuators cannot generate as much force as piezoelectric actuators, but there is substantial room for improvement. First, the $F_{\rm block}$ values are extrapolated from the linear region of the exponential curve. As Figure 8

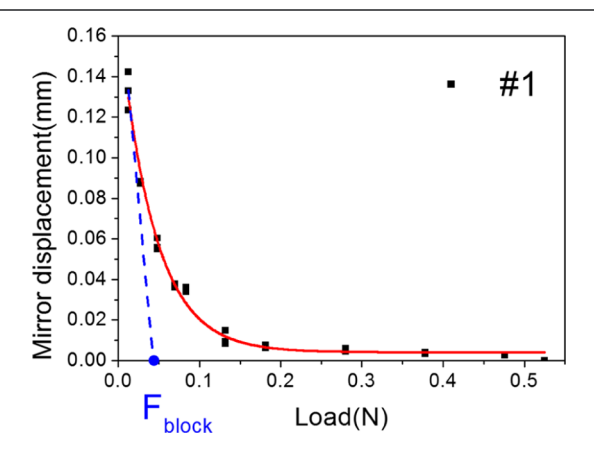


Figure 8. Plot of vertical displacement versus load for a typical DAE/AAO bending actuator (denoted #1, black squares), along with exponential fit (red line). A linear fit to the initial decay is shown in blue, along with the value of F_{block} extracted from this fit.

shows, the DAE/AAO actuator continues to generate displacement for values larger than $F_{\rm block}$. Second, it is likely that the high elastic modulus of the AAO resists the photomechanical motion of the organic and lowers the amount of useful work that can be extracted. It is likely that using a more compliant template or a photochemical reaction that generates more force can boost both ΔL_0 and $F_{\rm block}$. Third, the response time of several minutes seen in Figure 7b results from the low light intensities (5–10 mW/cm²) used in our experiments and does not represent an intrinsic limitation of the material. Because the displacement tracks the photochemical reaction, increasing the light intensity to 1 W/cm² should lead to response times of less than a second.

The photoinduced bending requires that the photomechanical crystals are correctly oriented inside the template so that the expansion occurs in the plane of the substrate. Different crystal orientations, lack of crystallinity, or incomplete filling of the channels can all suppress this effect. For example, although the majority (~80%) of our templates showed photomechanical responses that match those reported in Figures 4-8, the other 20% showed low or sometimes no photomechanical response at all. Usually the poorly performing samples suffered from poor loading, but we cannot rule out misdirected or random crystal growth. We tested two other photomechanical crystal materials, based on 1,2-bis(2,4dimethyl-5-phenyl-3-thienyl)perfluorocyclopentene⁵¹ and 4fluoro-9-anthracenecarboxylic acid, 52 but neither was able to generate photoinduced bending in the AAO template. Both molecules filled the channels, but we suspect that these crystals were not correctly oriented to generate stress across the horizontal plane of the template.

CONCLUSIONS

This work shows how ordering the organic-active component on both the molecular scale (by oriented crystal growth in each pore) and the macroscopic scale (by growing a regular array of crystalline nanowires in a porous inorganic template) can lead to a hybrid photomechanical material capable of moving macroscopic objects solely through light power. Very small (sub-milligram) amounts of material can move masses that are 10⁴ times larger without being physically connected to an external power source. Lowering the template elastic modulus and varying the organic photochrome are two future pathways to improve actuator performance. These proof-of-principle experiments illustrate a way to incorporate photomechanical molecular crystals into macroscopic actuator structures, potentially opening up new applications for these interesting materials.

ASSOCIATED CONTENT

S Supporting Information

The Supporting Information is available free of charge on the ACS Publications website at DOI: 10.1021/acs.chemmater.8b04568.

Additional information on sample preparation and characterization, and displacement calculations (PDF) Movies of the light-induced mirror motion (MPG) Movies of the laser beam displacement (MPG)

AUTHOR INFORMATION

Corresponding Authors

*E-mail: kitagawa@osaka-cu.ac.jp (D.K.).

*E-mail: kobatake@a-chem.eng.osaka-cu.ac.jp (S.K.).

*E-mail: christopher.bardeen@ucr.edu (C.J.B.).

ORCID (

Xinning Dong: 0000-0003-4728-6862 Fei Tong: 0000-0003-4545-2230

Kerry M. Hanson: 0000-0002-6942-3330 Daichi Kitagawa: 0000-0002-1994-3047 Seiya Kobatake: 0000-0002-1526-4629

Christopher J. Bardeen: 0000-0002-5755-9476

Author Contributions

The original idea of this project was conceived by C.J.B. Most of the experiment was performed by X.D. with help and

instructions by D.K. and F.T. The compound was synthesized by D.K. and S.K. The diffuse reflectance data was conducted by K.H. and X.D. Theoretical support was provided by R.O.K. and S.K. The draft of manuscript was written by C.J.B. with input of R.O·K., D.K. and X.D. All authors contributed to the discussion of final results.

Notes

The authors declare no competing financial interest.

ACKNOWLEDGMENTS

This research was supported by the National Science Foundation grant DMR-1810514 and by the MURI on Photomechanical Material Systems (ONR N00014-18-1-2624) (C.J.B.), by JSPS KAKENHI grant numbers JP15K21725, JP26107013 in Scientific Research on "Photosynergetics" (S.K.), by JSPS KAKENHI grant number JP16K17896 in Scientific Research for Young Scientists (B) (D.K.).

REFERENCES

- (1) Kim, T.; Zhu, L.; Al-Kaysi, R. O.; Bardeen, C. J. Organic photomechanical materials. *ChemPhysChem* **2014**, *15*, 400–414.
- (2) Han, D.-D.; Zhang, Y.-L.; Ma, J.-N.; Liu, Y.-Q.; Han, B.; Sun, H.-B. Light-Mediated Manufacture and Manipulation of Actuators. *Adv. Mater.* **2016**, 28, 8328–8343.
- (3) White, T. J. Photomechanical Materials, Composites, and Systems, 1 ed.; Wiley: Hoboken, New Jersey, 2017.
- (4) Ikeda, T.; Mamiya, J.-i.; Yu, Y. Photomechanics of liquid-crystalline elastomers and other polymers. *Angew. Chem., Int. Ed.* **2007**, *46*, 506–528.
- (5) Iamsaard, S.; Aßhoff, S. J.; Matt, B.; Kudernac, T.; Cornelissen, J. J. L. M.; Fletcher, S. P.; Katsonis, N. Conversion of Light into Macroscopic Helical Motion. *Nat. Chem.* **2014**, *6*, 229–235.
- (6) Naumov, P.; Chizhik, S.; Panda, M. K.; Nath, N. K.; Boldyreva, E. Mechanically Responsive Molecular Crystals. *Chem. Rev.* **2015**, 115, 12440–12490.
- (7) Kitagawa, D.; Kobatake, S. Crystal Thickness Dependence of Photoinduced Crystal Bending of 1,2-Bis(2-methyl-5-(4-(1-naphthoyloxymethyl)phenyl)-3-thienyl)perfluorocyclopentene. *J. Phys. Chem. C* **2013**, *117*, 20887–20892.
- (8) Kim, T.; Zhu, L.; Mueller, L. J.; Bardeen, C. J. Mechanism of photo-induced bending and twisting in crystalline microneedles and microribbons composed of 9-methylanthracene. *J. Am. Chem. Soc.* **2014**, *136*, 6617–6625.
- (9) Nath, N. K.; Pejov, L.; Nichols, S. M.; Hu, C.; Saleh, N. i.; Kahr, B.; Naumov, P. Model for photoinduced bending of slender molecular crystals. *J. Am. Chem. Soc.* **2014**, *136*, 2757–2766.
- (10) Boldyreva, E. V.; Sinelnikov, A. A.; Chupakhin, A. P.; Lyakhov, N. Z.; Boldyrev, V. V. Deformation and mechanical destruction of $[Co(NH_3)_5NO_2]X_2$ crystals (X = chloride, bromide, nitrate) during photostimulated linkage isomerization. *Dokl. Akad. Nauk* **1984**, 277, 893–896.
- (11) Naumov, P.; Kowalik, J.; Solntsev, K. M.; Baldridge, A.; Moon, J.-S.; Kranz, C.; Tolbert, L. M. Topochemistry and photomechanical effects in crystals of green fluorescent protein-like chromophores: effects of hydrogen bonding and crystal packing. *J. Am. Chem. Soc.* **2010**, *132*, 5845–5857.
- (12) Koshima, H.; Ojima, N.; Uchimoto, H. Mechanical motion of azobenzene crystals upon photoirradiation. *J. Am. Chem. Soc.* **2009**, 131, 6890–6891.
- (13) Koshima, H.; Takechi, K.; Uchimoto, H.; Shiro, M.; Hashizume, D. Photomechanical bending of salicylideneaniline crystals. *Chem. Commun.* **2011**, 47, 11423–11425.
- (14) Al-Kaysi, R. O.; Bardeen, C. J. Reversible photoinduced shape changes of crystalline organic nanorods. *Adv. Mater.* **2007**, *19*, 1276–1280.

(15) Bushuyev, O. S.; Singleton, T. A.; Barrett, C. J. Reversible, and General Photomechanical Motion in Single Crystals of Various Azo Compounds Using Visible Light. *Adv. Mater.* **2013**, 25, 1796–1800.

- (16) Bushuyev, O. S.; Tomberg, A.; Friščić, T.; Barrett, C. J. Shaping Crystals with Light: Crystal-to-Crystal Isomerization and Photomechanical Effect in Fluorinated Azobenzenes. *J. Am. Chem. Soc.* **2013**, *135*, 12556–12559.
- (17) Zhu, L.; Al-Kaysi, R. O.; Bardeen, C. J. Reversible photo-induced twisting of molecular crystal microribbons. *J. Am. Chem. Soc.* **2011**, *133*, 12569–12575.
- (18) Kitagawa, D.; Nishi, H.; Kobatake, S. Photoinduced twisting of a photochromic diarylethene crystal. *Angew. Chem., Int. Ed.* **2013**, *52*, 9320–9322.
- (19) Kitagawa, D.; Tsujioka, H.; Tong, F.; Dong, X.; Bardeen, C. J.; Kobatake, S. Control of Photomechanical Crystal Twisting by Illumination Direction. *J. Am. Chem. Soc.* **2018**, *140*, 4208–4212.
- (20) Al-Kaysi, R. O.; Müller, A. M.; Bardeen, C. J. Photochemically driven shape changes of crystalline organic nanorods. *J. Am. Chem. Soc.* **2006**, *128*, 15938–15939.
- (21) Garcia-Garibay, M. A. Molecular crystals on the move: From single-crystal-to-single-crystal photoreactions to molecular machinery. *Angew. Chem., Int. Ed.* **2007**, *46*, 8945–8947.
- (22) Koshima, H.; Matsudomi, M.; Uemura, Y.; Kimura, F.; Kimura, T. Light-driven Bending of Polymer Films in Which Salicylidenephenylethylamine Crystals are Aligned Magnetically. *Chem. Lett.* **2013**, 42, 1517–1519.
- (23) Lan, T.; Chen, W. Hybrid Nanoscale Organic Molecular Crystals Assembly as a Photon-Controlled Actuator. *Angew. Chem., Int. Ed.* **2013**, *52*, 6496–6500.
- (24) Sahoo, S. C.; Nath, N. K.; Zhang, L.; Semreen, M. H.; Al-Telb, T. H.; Naumov, P. Actuation Based on Thermo/Photosalient Effect: a Biogenic Smart Hybrid Driven by Light and Heat. *RSC Adv.* **2014**, *4*, 7640–7647.
- (25) Yu, Q.; Yang, X.; Chen, Y.; Yu, K.; Gao, J.; Liu, Z.; Cheng, P.; Zhang, Z.; Aguila, B.; Ma, S. Fabrication of Light-Triggered Soft Artificial Muscles via a Mixed-Matrix Membrane Strategy. *Angew. Chem., Int. Ed.* **2018**, *57*, 10192–10196.
- (26) Cölfen, H.; Mann, S. Higher-Order Organization by Mesoscale Self-Assembly and Transformation of Hybrid Nanostructures. *Angew. Chem., Int. Ed.* **2003**, 42, 2350–2365.
- (27) O'Brien, M. N.; Jones, M. R.; Mirkin, C. A. The Nature and Implications of Uniformity in the Hierarchical Organization of Nanomaterials. *Proc. Natl. Acad. Sci. U.S.A.* **2016**, *113*, 11717–11725.
- (28) Kobatake, S.; Takami, S.; Muto, H.; Ishikawa, T.; Irie, M. Rapid and reversible shape changes of molecular crystals on photo-irradiation. *Nature* **2007**, *446*, 778–781.
- (29) Terao, F.; Morimoto, M.; Irie, M. Light-driven molecular-crystal actuators: rapid and reversible bending of rodlike mixed crystals of diarylethene derivatives. *Angew. Chem., Int. Ed.* **2011**, *51*, 901–904.
- (30) Irie, M.; Fukaminato, T.; Matsuda, K.; Kobatake, S. Photochromism of Diarylethene Molecules and Crystals: Memories, Switches, and Actuators. *Chem. Rev.* **2014**, *114*, 12174–12277.
- (31) Irie, M.; Kobatake, S.; Horichi, M. Reversible Surface Morphology Changes of a Photochromic Diarylethene Single Crystal by Photoirradiation. *Science* **2001**, *291*, 1769–1772.
- (32) Morimoto, M.; Irie, M. A diarylethene cocrystal that converts light into mechanical work. *J. Am. Chem. Soc.* **2010**, *132*, 14172–14178.
- (33) Kuroki, L.; Takami, S.; Yoza, K.; Morimoto, M.; Irie, M. Photoinduced shape changes of diarylethene single crystals: correlation between shape changes and molecular packing. *Photochem. Photobiol. Sci.* **2010**, *9*, 221–225.
- (34) Ohshima, S.; Morimoto, M.; Irie, M. Light-Driven Bending of Diarylethene Mixed Crystals. *Chem. Sci.* **2015**, *6*, 5746–5752.
- (35) Kitagawa, D.; Kobatake, S. Photoreversible Current ON/OFF Switching by the Photoinduced Bending of Gold-Coated Diarylethene Crystals. *Chem. Commun.* **2015**, *51*, 4421–4424.

(36) Kitagawa, D.; Tanaka, R.; Kobatake, S. Photoinduced Stepwise Bending Behavior of Photochromic Diarylethene Crystals. *CrystEng-Comm* **2016**, *18*, 7236–7240.

- (37) Lee, W.; Park, S.-J. Porous Anodic Aluminum Oxide: Anodization and Templated Synthesis of Functional Nanostructures. *Chem. Rev.* **2014**, *114*, 7487–7556.
- (38) Al-Kaysi, R. O.; Bardeen, C. J. General method for the synthesis of crystalline organic nanorods using porous alumina templates. *Chem. Commun.* **2006**, 1224–1226.
- (39) Yamada, T.; Muto, K.; Kobatake, S.; Irie, M. Crystal Structure-Reactivity Correlation in Single-Crystalline Photochromism of 1,2-Bis(2-methyl-5-phenyl-3-thienyl)perfluorocyclopentene. *J. Org. Chem.* **2001**, *66*, 6164–6168.
- (40) Herder, M.; Schmidt, B. M.; Grubert, L.; Pätzel, M.; Schwarz, J.; Hecht, S. Improving the Fatigue Resistance of Diarylethene Switches. J. Am. Chem. Soc. 2015, 137, 2738–2747.
- (41) Cheng, L.; Torres, Y.; Lee, K. M.; McClung, A. J.; Baur, J.; White, T. J.; Oates, W. S. Photomechanical Bending Mechanics of Polydomain Azobenzene Liquid Crystal Polymer Network Films. *J. Appl. Phys.* **2012**, *112*, 013513–17.
- (42) Zhang, L.; Chizhik, S.; Wen, Y.; Naumov, P. Directed Motility of Hygroresponsive Biomimetic Actuators. *Adv. Funct. Mater.* **2015**, 26, 1040–1053.
- (43) Chizhik, S.; Sidelnikov, A.; Zakharov, B.; Naumov, P.; Boldyreva, E. Quantification of Photoinduced Bending of Dynamic Molecular Crystals: from Macroscopic Strain to Kinetic Constants and Activation Energies. *Chem. Sci.* **2018**, *9*, 2319–2335.
- (44) Liu, L.; Liu, M.-H.; Deng, L.-L.; Lin, B.-P.; Yang, H. Near-Infrared Chromophore Functionalized Soft Actuator with Ultrafast Photoresponsive Speed and Superior Mechanical Property. *J. Am. Chem. Soc.* **2017**, *139*, 11333–11336.
- (45) Loomis, J.; Panchapakesan, B. Dimensional Dependence of Photomechanical Response in Carbon Nanostructure Composites: a Case for Carbon-Based Mixed-Dimensional Systems. *Nanotechnology* **2012**, 23, 215501.
- (46) Loomis, J.; Fan, X.; Khosravi, F.; Xu, P.; Fletcher, M.; Cohn, R. W.; Panchapakesan, B. Graphene/Elastomer Composite-Based Photo-Thermal Nanopositioners. *Sci. Rep.* **2013**, *3*, 1900/1–10.
- (47) Serak, S.; Tabiryan, N.; Vergara, R.; White, T. J.; Vaia, R. A.; Bunning, T. J. Liquid Crystalline Polymer Cantilever Oscillators Fueled by Light. *Soft Matter* **2010**, *6*, 779–783.
- (48) Piezo Physik Instrumente Models. PL112 PL140 PICMA Bender. https://www.physikinstrumente.com/en/products/piezoceramic-actuators/bender-actuators/pl112-pl140-picma-bender-103000/#specification (accessed Jan.2, 2019).
- (49) Piezo Physik Instrumente Models. PD410 Round PICMA Multilayer Bender Actuators. https://www.physikinstrumente.com/en/products/piezoceramic-actuators/bender-actuators/pd410-round-picma-multilayer-bender-actuators-103050/#specification. (accessed Ian.2.2019).
- (50) Thorlabs. Piezoelectric Benders. PB4NB2W. https://www.thorlabs.com/newgrouppage9.cfm?objectgroup_id=10958. (accessed Jan.2,2019).
- (51) Tong, F.; Kitagawa, D.; Dong, X.; Kobatake, S.; Bardeen, C. J. Photomechanical motion of diarylethene molecular crystal nanowires. *Nanoscale* **2018**, *10*, 3393–3398.
- (52) Zhu, L.; Tong, F.; Salinas, C.; Al-Muhanna, M. K.; Tham, F. S.; Kisailus, D.; Al-Kaysi, R. O.; Bardeen, C. J. Improved Solid-State Photomechanical Materials by Fluorine Substitution of 9-Anthracene Carboxylic Acid. *Chem. Mater.* **2014**, *26*, 6007–6015.